Marí Soucase, B.; K.C. SINGH; Moya Forero, MM.; Hari Om (2014). Synthesis and down conversion emission property of Eu3+ doped LaAlO3 CsAlO2 and LiLaO2 phosphors. Optical and Quantum Electronics. 1-6. doi:10.1007/s11082-014-9997-9.

Springer

Dear Author,

Here are the proofs of your article.

- You can submit your corrections **online**, via **e-mail** or by **fax**.
- For **online** submission please insert your corrections in the online correction form. Always indicate the line number to which the correction refers.
- You can also insert your corrections in the proof PDF and **email** the annotated PDF.
- For fax submission, please ensure that your corrections are clearly legible. Use a fine black pen and write the correction in the margin, not too close to the edge of the page.
- Remember to note the **journal title**, **article number**, and **your name** when sending your response via e-mail or fax.
- **Check** the metadata sheet to make sure that the header information, especially author names and the corresponding affiliations are correctly shown.
- **Check** the questions that may have arisen during copy editing and insert your answers/ corrections.
- **Check** that the text is complete and that all figures, tables and their legends are included. Also check the accuracy of special characters, equations, and electronic supplementary material if applicable. If necessary refer to the *Edited manuscript*.
- The publication of inaccurate data such as dosages and units can have serious consequences. Please take particular care that all such details are correct.
- Please **do not** make changes that involve only matters of style. We have generally introduced forms that follow the journal's style.
  Substantial changes in content, e.g., new results, corrected values, title and authorship are not allowed without the approval of the responsible editor. In such a case, please contact the Editorial Office and return his/her consent together with the proof.
- If we do not receive your corrections **within 48 hours**, we will send you a reminder.
- Your article will be published **Online First** approximately one week after receipt of your corrected proofs. This is the **official first publication** citable with the DOI. **Further changes are, therefore, not possible.**
- The **printed version** will follow in a forthcoming issue.

Please note

After online publication, subscribers (personal/institutional) to this journal will have access to the complete article via the DOI using the URL: http://dx.doi.org/[DOI].
If you would like to know when your article has been published online, take advantage of our free alert service. For registration and further information go to: http://www.link.springer.com.

Due to the electronic nature of the procedure, the manuscript and the original figures will only be returned to you on special request. When you return your corrections, please inform us if you would like to have these documents returned.

Metadata of the article that will be visualized in OnlineFirst

Please note: Images will appear in color online but will be printed in black and white.

ArticleTitle	Synthesis and down conversion emission property of Eu^{3+} doped $LaAlO_3$, $CsAlO_2$ and $LiLaO_2$ phosphors	
Article Sub-Title		
Article CopyRight	Springer Science+Business Media New York (This will be the copyright line in the final PDF)	
Journal Name	Optical and Quantum Electronics	
Corresponding Author	Family Name	**Marí**
	Particle	
	Given Name	**B.**
	Suffix	
	Division	Institut de Disseny per la Fabricació Automatitzada (IDF) - Departament de Física Aplicada
	Organization	Universitat Politècnica de
	Address	València, Camí de Vera s/n, 46022, Valencia, Spain
	Email	bmari@fis.upv.es
Author	Family Name	**Singh**
	Particle	
	Given Name	**K. C.**
	Suffix	
	Division	Department of Chemistry
	Organization	Maharshi Dayanand University
	Address	124001, Rohtak, Haryana, India
	Email	
Author	Family Name	**Moya**
	Particle	
	Given Name	**M.**
	Suffix	
	Division	Institut de Disseny per la Fabricació Automatitzada (IDF) - Departament de Física Aplicada
	Organization	Universitat Politècnica de
	Address	València, Camí de Vera s/n, 46022, Valencia, Spain
	Email	
Author	Family Name	**Singh**
	Particle	
	Given Name	**Ishwar**
	Suffix	
	Division	Department of Chemistry
	Organization	Maharshi Dayanand University
	Address	124001, Rohtak, Haryana, India
	Email	
Author	Family Name	**Om**
	Particle	

	Given Name	**Hari**
	Suffix	
	Division	Department of Chemistry
	Organization	Maharshi Dayanand University
	Address	124001, Rohtak, Haryana, India
	Email	
Author	Family Name	**Chand**
	Particle	
	Given Name	**Subhash**
	Suffix	
	Division	Department of Chemistry
	Organization	Maharshi Dayanand University
	Address	124001, Rohtak, Haryana, India
	Email	

Schedule	Received	11 April 2014
	Revised	
	Accepted	29 July 2014

Abstract

$LaAlO_3$: Eu^{3+}, $CsAlO_2$: Eu^{3+} and $LiLaO_2$: Eu^{3+} phosphors with varying concentrations of Eu^{3+} from 3 to 10 mol% were prepared by combustion synthesis method and the samples were further heated to 1,000 °C to improve the crystallinity of the materials. The structure and morphology of materials have been examined by X-ray diffraction and scanning electron microscopy. SEM images depicted that the morphology of crystallites have no uniform shapes and sizes. Small and coagulated particles of irregular shapes of different sizes are obtained. The characteristic emissions of Eu^{3+} were clearly observed at nearly 580, 592, 650, 682 to 709 (multiplet structure) nm for $^5D_0 \rightarrow {}^7F_n$ transitions where $n = 0, 1, 3, 4$ respectively, including the strongest emission peaks at 614 and 620 nm for $^5D_0 \rightarrow {}^7F_2$ transitions in $CsAlO_2$: Eu^{3+} and $LiLaO_2$: Eu^{3+} host lattices. The intensity of emission peak corresponding to $^5D_0 \rightarrow {}^7F_1$ transitions in $LaAlO_3$: Eu^{3+} material is comparable to that of $^5D_0 \rightarrow {}^7F_2$ transitions which is also a singlet. Photoluminescence intensity follows the order as in $LiLaO_2 > LaAlO_3 > CsAlO_2$ lattices. Remarkable high photoluminescence intensity with 7 mol% doping of Eu^{3+} in $LiLaO_2$ makes it a strong contender for red colored display applications.

Keywords (separated by '-') Combustion synthesis - Phosphor materials - Down conversion - $LaAlO_3$: Eu^{3+} - $CsAlO_2$: Eu^{3+} - $LiLaO_2$: Eu^{3+}

Footnote Information

Opt Quant Electron
DOI 10.1007/s11082-014-9997-9

Synthesis and down conversion emission property of Eu^{3+} doped $LaAlO_3$, $CsAlO_2$ and $LiLaO_2$ phosphors

B. Marí · K. C. Singh · M. Moya · Ishwar Singh · Hari Om · Subhash Chand

Received: 11 April 2014 / Accepted: 29 July 2014

Abstract $LaAlO_3$:Eu^{3+}, $CsAlO_2$:Eu^{3+} and $LiLaO_2$:Eu^{3+} phosphors with varying concentrations of Eu^{3+} from 3 to 10 mol% were prepared by combustion synthesis method and the samples were further heated to 1,000 °C to improve the crystallinity of the materials. The structure and morphology of materials have been examined by X-ray diffraction and scanning electron microscopy. SEM images depicted that the morphology of crystallites have no uniform shapes and sizes. Small and coagulated particles of irregular shapes of different sizes are obtained. The characteristic emissions of Eu^{3+} were clearly observed at nearly 580, 592, 650, 682 to 709 (multiplet structure) nm for $^5D_0 \rightarrow {}^7F_n$ transitions where n = 0, 1, 3, 4 respectively, including the strongest emission peaks at 614 and 620 nm for $^5D_0 \rightarrow {}^7F_2$ transitions in $CsAlO_2$:Eu^{3+} and $LiLaO_2$:Eu^{3+} host lattices. The intensity of emission peak corresponding to $^5D_0 \rightarrow {}^7F_1$ transitions in $LaAlO_3$:Eu^{3+} material is comparable to that of $^5D_0 \rightarrow {}^7F_2$ transitions which is also a singlet. Photoluminescence intensity follows the order as in $LiLaO_2 > LaAlO_3 > CsAlO_2$ lattices. Remarkable high photoluminescence intensity with 7 mol% doping of Eu^{3+} in $LiLaO_2$ makes it a strong contender for red colored display applications.

Keywords Combustion synthesis · Phosphor materials · Down conversion · $LaAlO_3$:Eu^{3+} · $CsAlO_2$:Eu^{3+} · $LiLaO_2$:Eu^{3+}

1 Introduction

Rare-earth ions (Eu^{3+}, Sm^{3+}, Tb^{3+}, etc.) have been widely used as luminescent centers in phosphor materials due to their sharp 4f-intra shell transitions (Solovyev and Malkin

B. Marí (✉) · M. Moya
Institut de Disseny per la Fabricació Automatitzada (IDF) - Departament de Física Aplicada, Universitat Politècnica de, València, Camí de Vera s/n, 46022 Valencia, Spain
e-mail: bmari@fis.upv.es

K. C. Singh · I. Singh · H. Om · S. Chand
Department of Chemistry, Maharshi Dayanand University, Rohtak 124001, Haryana, India

Journal: 11082-OQEL Article No.: 9997 TYPESET DISK LE CP Disp.:2014/9/8 Pages: 10 Layout: Small

2007; Ogasawara et al. 2007; Shi et al. 1996). Among the rare-earth ions, europium is an attractive activator and has been used in phosphor materials for an efficient red and blue emission. The europium emission in the phosphor material is strongly dependent on the host lattice and it is possible to obtain different colors from blue to red. Europium can act as an activator in two forms, viz. Eu^{3+} and Eu^{2+}. Eu^{2+} or Eu^{3+} can be identified from their characteristic photoluminescence spectrum (Mao et al. 2009). For many years, optical properties of the trivalent europium (Eu^{3+}) doped crystals and glasses have been studied by numerous research groups. They have investigated Eu^{3+} emission in borates, oxides, silicates, phosphates, sulfates and fluorides (Zhang et al. 2012; Bae et al. 2009; Zhou and Yan 2008; Huang et al. 2009; Kijima et al. 2008; Kharbache et al. 2009). These materials find their applications in lighting, information display, and optoelectronics technology. The photoluminescence properties of RE-doped compounds not only depend on the composition and local structure of the host but also are affected by its crystal size and morphology.

It is our main interest to synthesize yet another family of newly developed Eu^{3+} doped phosphors via low temperature initiated combustion process and investigate their photoluminescence properties in view of the commercial importance of reddish-orange color emitting phosphors. The emission and absorption spectra of $LaAlO_3$:Eu^{3+} nanocrystals have been investigated and a detailed mechanism of luminescence has been proposed in literature by many researchers (Dereń and Krupa 2003; Hreniak et al. 2006). The mixed emission consisting of Eu^{2+} and Eu^{3+} in $LaAlO_3$ has been reported by Mao et al. (2009). There are very few references about the luminescence properties of $CsAlO_2$:Eu^{3+} and $LiLaO_2$:Eu^{3+} phosphors though their crystal structures are identified in literature (Perez and Vegas 2003; Pieterson et al. 2000). The structure of $CsAlO_2$ has been interpreted in the light of Zintl-Klemn concept as if the alkali metal atoms would donate electrons to the Al atoms. The compounds of stoichiometry $MAlO_2$ crystallize as stuffed cristobalites in which the Al array adopts the diamond like structure of Si (Perez and Vegas 2003). The $LiLaO_2$ material is found to have α-$NaFeO_2$-related crystal structure (Pieterson et al. 2000). But Abbattista and Vallino (1983) have concluded from the study of the La_2O_3–Li_2O binary system between 750 and 1,000 °C that $LaLiO_2$ occurs as the only binary compound. It is characterized by a monoclinic cell ($a_0 = 5.88$ Å; $b_0 = 6.22$ Å; $c_0 = 5.84$ Å; $\beta = 102.53°$) and is isomorphous with $\alpha - EuLiO_2$. Any orthorhombic polymorph of this compound is excluded between 750 and 1,000 °C.

As known, different material preparation methods have some important effects on material microstructure and physical properties. The combustion synthesis method had been earlier used by us to prepare phosphor materials consisting of ZrO_2, $BaZrO_3$ and MLn_2O_4 (M=Ba or Sr, Ln=Gd or La) doped with Eu^{3+} and Tb^{3+} ions (Marí et al. 2010; Marí and Singh 2013). This method provides an interesting alternative over other elaborated techniques because it offers several attractive advantages such as: simplicity of experimental set-up; surprisingly short time between the preparation of reactants and the availability of the final product; and being cheap due to energy saving. The main point of this method is the rapid decomposition of the rare earth nitrate in the presence of an organic fuel. During the reaction, many gases, such as CO_2, N_2, NO_2 and H_2O as well as a large amount of heat are released in a short period of time before the process terminates with white, foamy and crisp products. Many times final products are found to be composed of nanosized particles (Ekambaram and Patil 1997). This work has been carried out with the aim to prepare and compare the down conversion property of nanosized crystalline powders of $LaAlO_3$, $CsAlO_2$ and $LiLaO_2$ doped with Eu^{3+} and sintered at a temperature of 1,000 °C. The crystalline structure, morphology of particles and their photoluminescence properties are characterized by XRD, SEM and emission spectra under 325 nm laser excitation.

Journal: 11082-OQEL Article No.: 9997 TYPESET DISK LE CP Disp.:2014/9/8 Pages: 10 Layout: Small

2 Expérimental

High purity $CsNO_3$, $LiNO_3$, $[Al(NO_3)_3]$, $[La(NO_3)_3]$, $[Eu(NO_3)_3]$, H.M.T.A. (Hexa Methylene Tetra Amine) and carbohydrazide from Aldrich chemicals were taken as starting materials. Carbohydrazide was used as a fuel for preparation of $CsAlO_2$:Eu^{3+} phosphors while H.M.T.A. was used for synthesis of $LaAlO_3$:Eu^{3+}, and $LiLaO_2$:Eu^{3+} powders. Eu^{3+} doped nanocrystals with general formula $CsAl_{(1-x)}O_2$:xEu^{3+}, $La_{(1-x)}AlO_3$:xEu^{3+} and $Li\,La_{(1-x)}O_2$:xEu^{3+} where x varies from 3 to 10 mol%, were prepared by heating rapidly an aqueous concentrated paste containing a calculated amount of metal nitrates and a fuel in a preheated furnace maintained at 500 °C. The amount of fuel was calculated using total oxidizing and reducing valences (Ekambaram and Patil 1997). (1−x) moles of $[Al(NO_3)_3]$ were taken for preparation of $CsAl_{(1-x)}O_2$:xEu^{3+} phosphor while for $La_{(1-x)}AlO_3$:xEu^{3+} and $LiLa_{(1-x)}O_2$:xEu^{3+} materials preparation, (1-x) moles of $[La(NO_3)_3]$ were used. The material undergoes rapid dehydration and foaming followed by decomposition, generating combustible gases. These volatile combustible gases ignite and burn with a flame, yielding a voluminous solid. The combustion process utilizes the enthalpy of combustion for the formation and the obtained solid was again annealed at 1,000 °C for 3 h to increase crystallinity and photo luminescence intensity.

The morphology of the crystals was studied by scanning electron microscopy (SEM) using JEOL JSM6300 scanning electron microscope operating at 10 kV. Photoluminescence (PL) experiments were performed in backscattering geometry using a He–Cd laser (325 nm) with an optical power of 30 mW for excitation. The emitted light was analyzed by HR-4000 Ocean Optics USB spectrometer optimized for the UV–Vis range. For the photoluminescence measurement, 0.05 g powder samples were pressed into pellets (10 mm diameter and 1 mm thickness) and then exposed to a UV laser at 325 nm. All measurements were carried out at room temperature. The structural characterization was done by a high resolution X-ray diffraction (XRD) using a Rigaku Ultima IV diffractometer in the θ–2θ configuration and using Cu Kα radiation (1.5418 Å).

The Scherrer equation:

$$\tau = \frac{K\lambda}{\beta \cos\theta}$$

where:

- τ is the mean size of the ordered (crystalline) domains, which may be smaller or equal to the grain size;
- K is a dimensionless shape factor, with a value close to unity. The shape factor has a typical value of about 0.9, but varies with the actual shape of the crystallite;
- λ is the X-ray wavelength;
- β is the line broadening at half the maximum intensity (FWHM), after subtracting the instrumental line broadening, in radians. This quantity is sometimes denoted as $\Delta(2\theta)$;
- θ is the Bragg angle.

was used to calculate the crystallite size of all materials. At least five prominent peaks from each XRD (samples with various Eu^{3+} concentration) were used for calculation and peaks belonging to different phases were also taken into consideration. Maximum and minimum values obtained for each type of lattice are reported as range of crystallite size (e.g. 30–40 nm for $LaAlO_3$).

Journal: 11082-OQEL Article No.: 9997 TYPESET DISK LE CP Disp.:2014/9/8 Pages: 10 Layout: Small

3 Results and discussions

3.1 XRD studies

Figure 1a–c shows the X-ray diffractograms of Eu^{3+} doped $LaAlO_3$, $CsAlO_2$ and $LiLaO_2$ powders. The phase analysis demonstrates that $LaAlO_3$:Eu^{3+} belongs to trigonal crystal system with R3 m (160) space group having unit cell dimensions: $a = b = 5.364$ Å and $c = 13.11$ Å (Fig. 1a). This is in good agreement with the standard JCPDS files No. 031-0022. In this phosphor, trivalent lanthanum ions are replaced by trivalent europium ions. Dopant ions (Eu^{3+}) concentration variation from 3 to 20 mol% have no noticeable effect on the obtained X-ray diffractograms of the as-prepared $LaAlO_3$:Eu^{3+} phosphors, indicating that the doped ions occupied the primordial La^{3+} sties. However, the XRD patterns of, Eu^{3+}doped $LiLaO_2$ and $CsAlO_2$ phosphors show the presence of two and three phases respectively. In Fig. 1c the XRD spectra show the presence of orthorhombic $LiLaO_2$ (JCPDS No. 019-0722) and hexagonal La_2O_3 (JCPDS No. 005-0602) crystalline phases in $LiLaO_2$:Eu^{3+} powders. The presence of orthorhombic $LiLaO_2$ phase is contrary to the monoclinic phase as observed by Abbattista and Vallino (1983). With the increase of dopant concentration of Eu^{3+} separation of La_2O_3 phase becomes more evident. Intensity of diffraction peaks corresponding to $LiLaO_2$ phase decreases and La_2O_3 phase increases with the increase of Eu^{3+} concentration. The presence of La_2O_3 phase also indicates that Eu^{3+} ions are preferred in $LiLaO_2$ lattice than that of La^{3+} ions. Taking into account the radii fit of ions involved in the host lattice, the substitution of Eu^{3+}(0.109 nm) for La^{3+}(0.117 nm) is preferred since there is large radii difference between Li^{+}(0.090 nm) and La^{3+}(0.117 nm) which may cause more strain. The absence of any cluster phase like Eu_2O_3 at all doping concentrations of Eu^{3+} ions shows the substitution of all Eu^{3+} ions in $LiLaO_2$ lattice is complete.

The XRD patterns of $CsAlO_2$:Eu^{3+} powders are compared in Fig. 1b. The presence of three crystalline phases $Cs_2O!11Al_2O_3$ (JCPDS No. 023-0883), $Cs_2O!Al_2O_3$ (JCPDS No. 023-0882) and Cs_2O_3 (JCPDS No. 010-0248) belonging to hexagonal and cubic crystal systems are detected. Cs_2O_3 phase is more prominent at low doping concentrations of Eu^{3+}, but $Cs_2O!11Al_2O_3$ phase is more favorable at higher Eu^{3+} concentrations. The ionic radius of Eu^{3+} (0.109 nm) ions is lying between the ionic radii of Cs^{+}(0.181 nm) and Al^{3+}(0.0675 nm) ions, therefore its substitution for former will cause distortion in lattice parameters as well as charge imbalance, while for the latter it will cause only distortion. The substitution of Cs+ ions with Eu^{3+} ions has to be accompanied by the creation of some defect in lattice for charge balance. These defects may facilitate the radiationless transfer of energy, thus affecting the luminescence intensity of the phosphor. Again the absence of any cluster phase of Eu_2O_3 at all doping concentrations shows the substitution of all Eu^{3+} ions in $CsAlO_2$ lattice is successful.

3.2 SEM micrograph and particle size analysis

Crystallinity, particle size and surface roughness of the phosphor have strong effects on the photoluminescence. Figure 2a–f exhibit surface morphologies of Eu^{3+} doped $LaAlO_3$, $CsAlO_2$ and $LiLaO_2$ particles. It is clear from SEM images that the morphologies of crystallites have no uniform shapes and sizes. Generally non- uniformity of shape and size is associated with the non-uniform distribution of temperature and mass flow in the combustion flame. Several pores are observed in SEM images (Fig. 2b) which are formed by the escaping gases during the combustion reaction. Also, several small particles can be seen within grains. Above mentioned features are inherent in combustion

Journal: 11082-OQEL Article No.: 9997 TYPESET DISK LE CP Disp.:2014/9/8 Pages: 10 Layout: Small

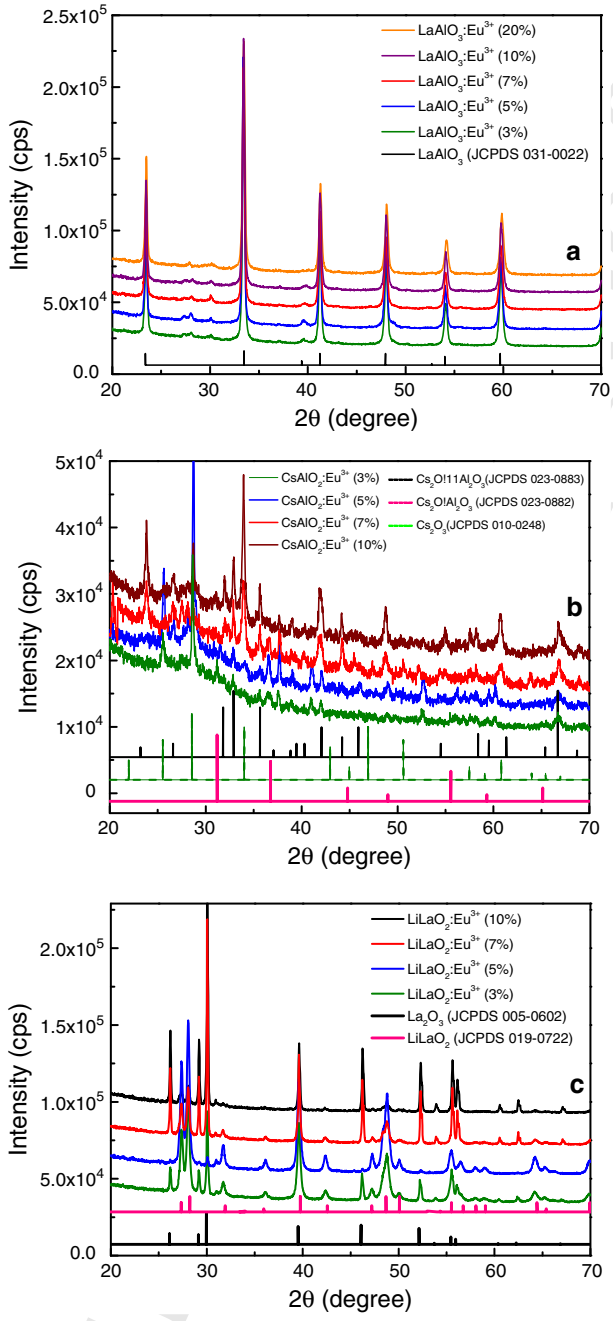

Fig. 1 X-ray diffractograms (XRD) of the Eu^{3+} doped **a** $LaAlO_3$, **b** $CsAlO_2$ and **c** $LiLaO_2$ crystals

derived powders. The SEM images of $CsAlO_2$:Eu^{3+} particles (Fig. 2e, f) and $LiLaO_2$:Eu^{3+} lattices (Fig. 2c, d) show that small and coagulated particles of irregular shapes of different sizes are obtained. However, the surface morphology of $LiLaO_2$:Eu^{3+} particles is

Journal: 11082-OQEL Article No.: 9997 TYPESET DISK LE CP Disp.:2014/9/8 Pages: 10 Layout: Small

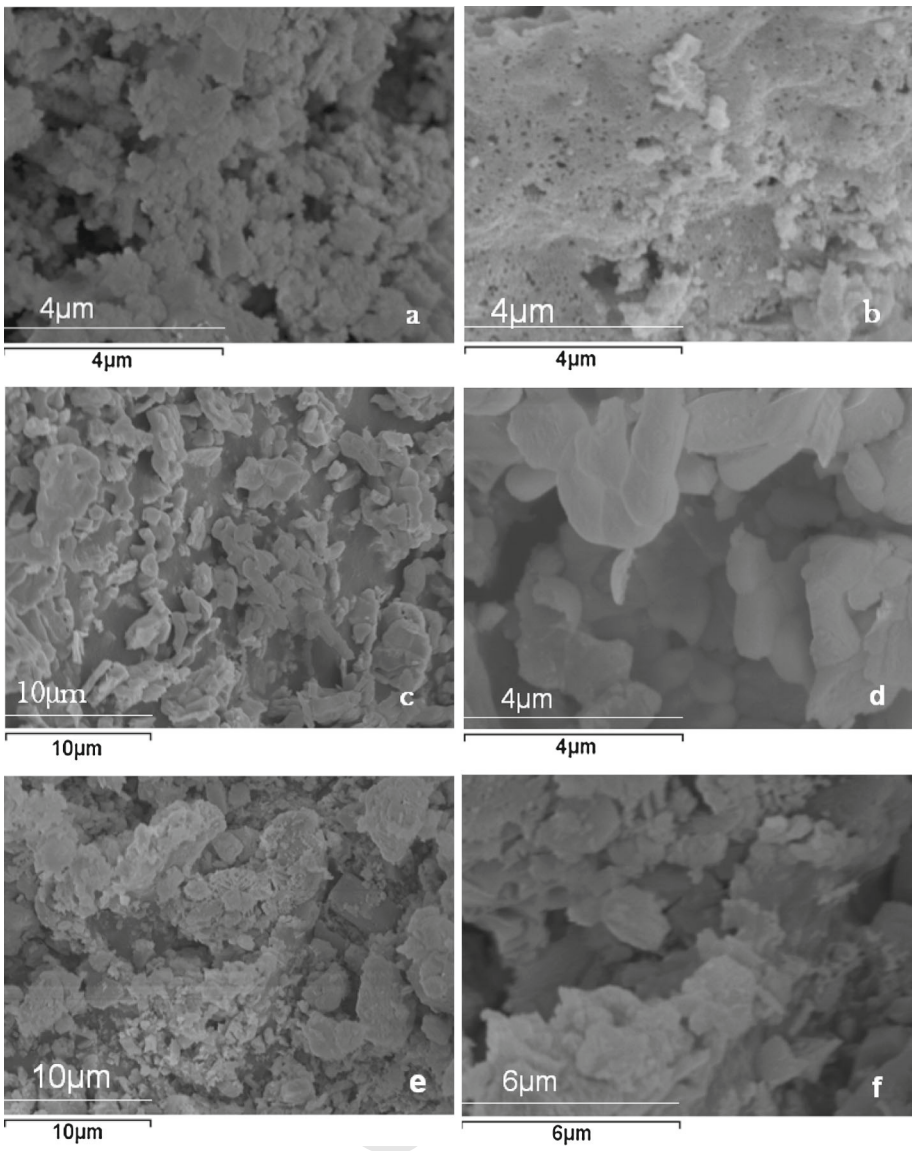

Fig. 2 SEM micrographs of particles **a**, **b** $LaAlO_3:Eu^{3+}$ **c**, **d** $LiLaO_2:Eu^{3+}$ and **e**, **f** $CsAlO_2:Eu^{3+}$

smooth. The smooth surface of phosphor free of defects can reduce the non-radiation and scattering resulted from coarse surface, thus beneficial to the luminescence efficiency in application (Liu 2007). The dense packed small particles can prevent the phosphors from aging. The average particle size as calculated from the Scherrer equation for $LaAlO_3$, $CsAlO_2$ and $LiLaO_2$ crystallites varies between 30–40, 40–70 and 26–30 nm, respectively.

Journal: 11082-OQEL Article No.: 9997 TYPESET DISK LE CP Disp.:2014/9/8 Pages: 10 Layout: Small

Table 1 The exact positions of emission peaks in various lattices

Lattice	$^5D_0 \rightarrow F_0$	$^5D_0 \rightarrow F_1$	$^5D_0 \rightarrow F_2$	$^5D_0 \rightarrow F_3$	$^5D_0 \rightarrow F_4$
$CsAlO_2:Eu^{3+}$	577	588–593	612–618	649	682–701
$LaAlO_3:Eu^{3+}$	581	592	617	649	684–691 700–705–709
$LiLaO_2:Eu^{3+}$	580	588–596	613–625	653	685–694–708

3.3 Photoluminescence properties

The room temperature emission spectra of Eu^{3+} doped $LaAlO_3$, $CsAlO_2$ and $LiLaO_2$ crystals with different doping concentrations are shown in Fig. 3a–c. The UV light of 325 nm is used for excitation of the luminescence. The obtained products emitted the red luminescence of varying intensities, which showed the activator Eu^{3+} has successfully entered the host lattice of $LaAlO_3$, $CsAlO_2$ and $LiLaO_2$. The characteristic emissions of Eu^{3+} were clearly observed with sharp and strong peaks at 614 and 620 nm for $^5D_0 \rightarrow {}^7F_2$ transition, and others at nearly 580, 592, 654, 705 nm for $^5D_0 \rightarrow {}^7F_n$ transitions where $n = 0, 1, 3, 4$ respectively. The exact positions of emission peaks in various lattices are shown in Table 1. The $^5D_0 \rightarrow {}^7F_1$ transition is well known to be mainly a magnetic dipole transition when the Eu^{3+} ions locate in a high symmetric position while the $^5D_0 \rightarrow {}^7F_{2,4}$ transitions are essentially electric dipole transitions which appear dominantly only when Eu^{3+} ion locates at sites without inversion symmetry (Ningthoujam et al. 2007; Gao et al. 2008).

In Fig. 3a, the emission intensity of all peaks rises with increase of doping concentration from 3 to 5 % and then starts decreasing. It becomes nearly one fifth with 20 % doping of Eu^{3+} in $LaAlO_3:Eu^{3+}$ phosphors. It is expected that with the increase of Eu^{3+} ions, photoluminescence should increase. However, the emission intensity decreases above 5 mol% of Eu^{3+} ions due to concentration quenching, because of non-radiative interaction between ions, the resonant energy transfer becomes stronger. As the concentration is increased, the Eu^{3+} ions are packed closer and closer together, which favors the transfer of energy from one europium ion to the next by a resonance process; the energy eventually reaches a trap from which it is dissipated by non-radiative processes rather than by the emission of visible light (Perea et al. 1998; Hayakawa et al. 1996). In the present investigation, the intensity of $^5D_0 \rightarrow {}^7F_1$ transition at 591 nm is comparable to $^5D_0 \rightarrow {}^7F_2$ transition at 616 nm. It may be mentioned that a similar behavior of magnetic dipole transition ($^5D_0 \rightarrow {}^7F_1$) was observed for Eu^{3+} doped LaAlO3 host (Kharbache et al. 2009; Dereń and Krupa 2003; Hreniak et al. 2006). In some cases, the magnetic dipole transition is stronger (Singh 2011), in others the electric dipole transition dominates (Mączka et al. 2012). Other weak intensity peaks are seen on either side of strong peaks. The two weak emission peaks at 536 and 557 nm are due to $^5D_2 \rightarrow {}^7F_3$ and $^5D_1 \rightarrow {}^7F_2$ transitions as reported in reference (Mao et al. 2010). The intensity ratio of 591 nm peak to 616 nm peak is a measure of asymmetry of the Eu^{3+} site in the host lattice (Blasse and Grambier 1994). The orange-red emission of the prepared $LaAlO_3:Eu^{3+}$ phosphor was proposed for its probable utility for display applications.

The emission spectra of $CsAlO_2$ and $LiLaO_2$ as shown in Fig. 3b, c also exhibit the concentration quenching effect of Eu^{3+} above 7 mol% doping. However the emission peaks at 614 and 620 nm for $^5D_0 \rightarrow {}^7F_2$ transitions are the strongest and small triplet of low intensity near 590 nm corresponding to $^5D_0 \rightarrow {}^7F_1$ transitions depicts the occupancy of Eu^{3+} ions at the low symmetry sites in $CsAlO_2$ and $LiLaO_2$ lattices. The comparison of

Journal: 11082-OQEL Article No.: 9997 TYPESET DISK LE CP Disp.:2014/9/8 Pages: 10 Layout: Small

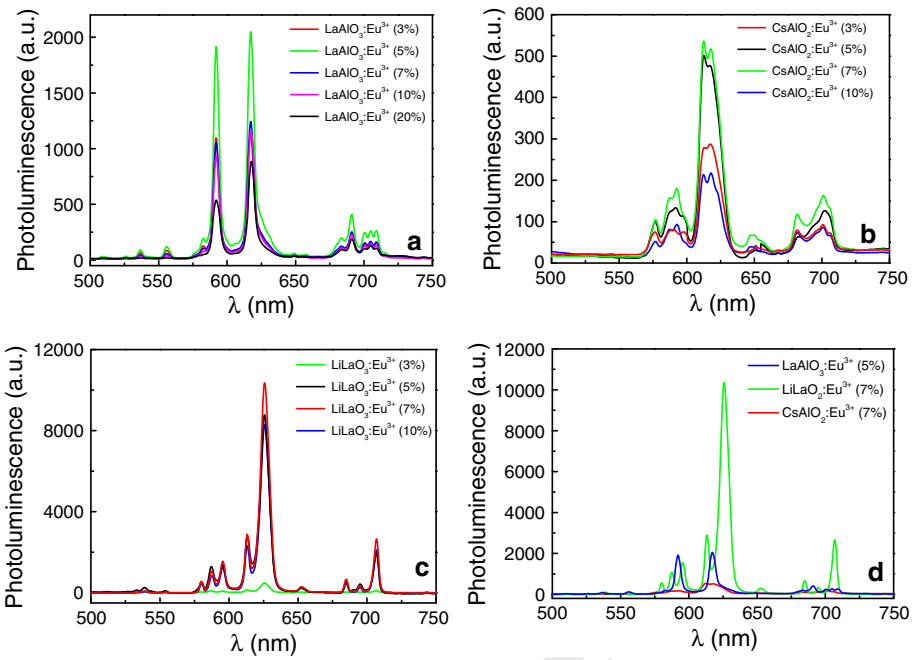

Fig. 3 Photoluminescence spectra of Eu^{3+} doped **a** $LaAlO_3$, **b** $CsAlO_2$, **c** $LiLaO_2$ phosphors with different doping concentrations and **d** comparison of luminescence spectra of $LaAlO_3$:Eu^{3+} (5 %), $CsAlO_2$:Eu^{3+} (7 %) and $LiLaO_2$:Eu^{3+} (7 %)

emission spectra of Eu^{3+} doped $LaAlO_3$, $CsAlO_2$ and $LiLaO_2$ phosphors as shown in Fig. 3d reveals the increase of nearly 450 % luminescence intensity of $LiLaO_2$:Eu^{3+} and decrease of 25 % of $CsAlO_2$:Eu^{3+} intensity in comparison to $LaAlO_3$:Eu^{3+} phosphor. Low emission intensity of Eu^{3+} ions in $CsAlO_2$ may be due to lack of energy transfer from Cs+ or Al^{3+} ions to Eu^{3+} ions or due to the presence of some surface impurities or surface defects. The smooth morphology and compact packing of $LiLaO_2$:Eu^{3+} particles as compare to $CsAlO_2$:Eu^{3+}or $LaAlO_3$:Eu^{3+} particles as depicted in SEM images may be a contributory factor for high luminescence intensity of $LiLaO_2$:Eu^{3+} samples. The $LiLaO_2$:Eu^{3+} material showing very high red luminescence of nearly 620 nm is definitely a material for further investigation for its use in display applications.

4 Conclusion

$LaAlO_3$:Eu^{3+}, $CsAlO_2$:Eu^{3+}, and $LiLaO_2$:Eu^{3+} powders were prepared by combustion synthesis method and the samples were further heated to 1,000 °C to improve the crystallinity of the materials. XRD analysis demonstrated that $LaAlO_3$:Eu^{3+} belonged to trigonal crystal system. Two and three phases were present in $LiLaO_2$:Eu^{3+} and $CsAlO_2$:Eu^{3+} powders respectively. The presence of orthorhombic $LiLaO_2$ and hexagonal La_2O_3 crystalline phases was detected in $LiLaO_2$:Eu^{3+} powders while three crystalline phases $Cs_2O!11Al_2O_3$, $Cs_2O!Al_2O_3$ and Cs_2O_3 belonging to hexagonal and cubic crystal systems were present in $CsAlO_2$:Eu^{3+} materials. The SEM images of crystallites showed small and coagulated particles of irregular shapes of different sizes. However, the surface morphology of

Journal: 11082-OQEL Article No.: 9997 TYPESET DISK LE CP Disp.:2014/9/8 Pages: 10 Layout: Small

$LiLaO_2:Eu^{3+}$ particles was smooth. The emission peaks at 614 and 620 nm for $^5D_0 \rightarrow {}^7F_2$ transitions were strongest for $CsAlO_2:Eu^{3+}$, and $LiLaO_2:Eu^{3+}$ materials. However, the intensity of $^5D_0 \rightarrow {}^7F_1$ transition at 591 nm was comparable to $^5D_0 \rightarrow {}^7F_2$ transition at 616 nm in $LaAlO_3:Eu^{3+}$ powder. The $LiLaO_2:Eu^{3+}$ material showing very high red luminescence of nearly 620 nm is definitely a material for further investigation for its use in display applications.

References

Abbattista, F., Vallino, M.: Remarks on the $La_2O_3 - Li_2O$ binary system between 750 and 1,000 °C. Ceram. Int. **9**, 35–38 (1983)

Bae, Y., Lee, K., Byeon, S.: Synthesis and Eu^{3+} concentration-dependent photoluminescence of $Gd_{2-x}Eu_xO_3$ nanowires. J. Lumin. **129**, 81–85 (2009)

Blasse, G., Grambier, B.: Luminescent Materials, vol. 43. Springer, Berlin, pp. 43–46 (1994)

Dereń, P., Krupa, J.: Spectroscopic investigations of $LaAlO_3:Eu^{3+}$. J. Lumin. **102–103**, 386–390 (2003)

Ekambaram, S., Patil, K.: Synthesis and properties of Eu^{2+} activated blue phosphors. J. Alloys Compd. **248**, 7–12 (1997)

Gao, X., Lei, L., Lv, C., Sun, Y., Zheng, H., Cui, Y.: Preparation and photoluminescence property of a loose powder, $Ca_3Al_2O_6:Eu^{3+}$ by calcination of a layered double hydroxide precursor. J. Solid State Chem. **181**, 1776–1781 (2008)

Hayakawa, T., Kamt, N., Yamada, K.: Visible emission characteristics in Tb^{3+}-doped fluorescent glasses under selective excitation. J. Lumin. **68**, 179–186 (1996)

Hreniak, D., Strek, W., Dereń, P., Bednarkiewicz, A., Łukowiak, A.: J. Alloys Compd. **408**, 828–830 (2006)

Huang, Y., Jiang, C., Cao, Y., Shi, L., Seo, H.: Luminescence and microstructures of Eu^{3+}-doped in triple phosphate $Ca_8MgR(PO_4)_7$ (R = La, Gd, Y) with whitlockite structure. Mater. Res. Bull. **44**, 793–798 (2009)

Kharbache, H., Mahiou, R., Boutinaud, P., Boyer, D., Zakaria, D., Deren, P.: Experimental evidence of Eu^{3+} pairs in K_2EuF_5. Opt. Mater. **31**, 558–561 (2009)

Kijima, T., Shinbori, T., Sekita, M., Uota, M., Sakai, G.: Abnormally enhanced Eu^{3+} emission in $Y_2O_2SO_4:Eu^{3+}$ inherited from their precursory dodecylsulfate-templated concentric-layered nanostructure. J. Lumin. **128**, 311–316 (2008)

Liu, G., Hong, G., Wang, J., Dong, X.: Hydrothermal synthesis of spherical and hollow $Gd_2O_3:Eu^{3+}$ phosphors. J. Alloys Compd. **432**, 200–204 (2007)

Mączka, M., Bednarkiewicz, A., Mendoza-Mendoza, E., Fuentes, A.F., Kępiński, L.: Optical properties of Eu and Er doped $LaAlO_3$ nanopowders prepared by low-temperature method. J. Solid State Chem. **194**, 264–269 (2012)

Mao, Z., Wang, D., Lu, Q., Yu, W., Yuan, Z.: Tunable single-doped single-host full-color-emitting $LaAlO_3$:Eu phosphor via valence state-controlled means. Chem. Commun. **3**, 346–348 (2009)

Mao, Z.Y., Wang, D.J., Liu, Y.H., Fei, Q.N., Zheng, X., Xu, S.C., Qiu, K.: Tuning the color purity of $LaAlO_3:Eu^{3+}$ red phosphor by the cross relaxation. Opto Electron. Lett. **6**, 116–119 (2010)

Marí, B., Singh, K., Sahal, M., Khatkar, S., Taxak, V., Kumar, M.: Preparation and luminescence properties of Tb^{3+} doped ZrO_2 and $BaZrO_3$ phosphors. J. Lumin. **130**, 2128–2132 (2010)

Marí, B., Singh, K.C., Cembrero-Coca, P., Singh, I., Singh, D., Chand, S.: Red emitting $MTiO_3$ (M = Ca & Sr) phosphor doped with Eu^{+3} or Pr^{+3} with some cations as co-dopands. Displays **34**, 346–351 (2013)

Ningthoujam, R., Sudarsan, V., Kulshreshtha, S.: SnO_2:Eu nanoparticles dispersed in silica: A low-temperature synthesis and photoluminescence study. J. Lumin. **127**, 747–756 (2007)

Ogasawara, K., Watanabe, S., Toyoshima, H., Brik, M.G.: Handbook on Physics and Chemistry of Rare Earths, vol. 1. Elsevier, Amsterdam (2007)

Pereyra-Perea, E., Estrada-Yañez, M.R., García, M.: Preliminary studies on luminescent terbium-doped ZrO2 thin films prepared by the sol-gel process. J. Phys. D **31**, 7–10 (1998)

Perez, D., Vegas, A.: The Zintl-Klemm concept applied to cations in oxides. I. The structures of ternary aluminates. Acta Cryst. B **59**, 305–323 (2003)

Pieterson, L., Heeroma, M., Heer, E., Meijerink, A.: Charge transfer luminescence of Yb^{3+}. J. Lumin. **91**, 177–193 (2000)

Shi, C., Shi, J., Deng, J., Han, Z., Zhou, Y., Zhang, G.: Excitation states of RE^{3+}-pentaphosphates in VUV and UV range. J. Electron. Spectros. Relat. Phenomena **79**, 121–124 (1996)

Journal: 11082-OQEL Article No.: 9997 TYPESET DISK LE CP Disp.:2014/9/8 Pages: 10 Layout: Small

279 Singh, V., Watanabe, S., Gundu Rao, T.K., Chubaci, J.F.D., Kwak, H.-Y.: Characterization, photoluminescence,
280 thermally stimulated luminescence and electron spin resonance studies of Eu^{3+} doped $LaAlO_3$ phosphor.
281 Solid State Sci. **13**, 66–71 (2011)
282 Solovyev, O.V., Malkin, B.Z.: Modeling of electron-vibrational $4f^n - 4f^{n-1}5d$ spectra in $LiYF_4:RE^{3+}$ crystals.
283 J. Mol. Struct. **838**, 176–181 (2007)
284 Zhang, Y., Li, W., Jingjun, X.: Structure and photoluminescence properties of $KSr_4(BO_3)_3:Eu^{3+}$ red-emitting
285 phosphor. Opt. Mater. Express **2**(2012), 92–102 (2012)
286 Zhou, L., Yan, B.: Sol-gel synthesis and photoluminescence of $CaSiO_3:Eu^{3+}$ nanophosphors using novel
287 silicate sources. J. Phys. Chem. Solids **69**, 2877–2882 (2008)

Journal: 11082-OQEL Article No.: 9997 TYPESET DISK LE CP Disp.:2014/9/8 Pages: 10 Layout: Small